Journal of Energy and Power Engineering 10 (2016) 313-323
doi: 10.17265/1934-8975/2016.05.006

Analysis and Prototyping of Multicellular DC-DC Transformer for Environmentally Friendly Data Centers

Yusuke Hayashi and Tamotsu Ninomiya

Power Electronics Circuits and Systems Laboratory, Green Electronics Research Institute, Kitakyushu, Fukuoka 808-0135, Japan

Received: March 02, 2016 / Accepted: March 15, 2016 / Published: May 31, 2016.

Abstract: A multicellular DCX (dc-dc transformer) using unregulated cell converters has been proposed for the environmentally friendly data centers. The high speed cell converter with the switching frequency over MHz behaves as an ideal transformer, and this behavior solves the voltage imbalance issue in the multicellular converter topology. The analysis of the unregulated cell converter is conducted by using the state space averaging method, and the operation condition for the ideal transformer is specified. The behavior of the multicellular DCX using the high speed cell converters has been also analyzed, and the voltage imbalance issue among cell converters is discussed quantitatively. A prototype of a 19.2 kW 384 V-384 V multicellular DCX using sixty-four unregulated cell converters is fabricated and the validity of the analyses is verified.

Key words: DCX (dc-dc transformer), high frequency dc-dc converter, ISOP (input series output parallel), IPOS (input parallel output series), state space averaging method.

1. Introduction

The amount of network traffic in the data centers has recently been rapidly increasing due to the widespread use of ICT (information and communication technology) equipment [1, 2]. Energy conservation and resource saving in data centers will contribute to solving some of our global environmental problems. NTT (Nippon Telegraph and Telephone) Group has been proposing a next generation dc (direct current) distribution system, that goes beyond the conventional 380 V dc distribution system to realize the highly electrified low carbon society [3-5].

One of features of the proposed dc distribution system is the effective utilization of the renewable energy sources. The highly efficient and the highly scalable DCX (dc-dc transformer) is the only component to interface various voltage levels of the energy storage devices and the renewable energy sources flexibly. The multicellular converter topology based on the ISOP (input series output parallel) IPOS (input parallel output series) connection of low voltage low power cell converters is one of options to realize the high scalable DCX.

In this paper, the multicellular DCX using unregulated cell converters is proposed. The cell converter with no voltage regulation is applied to the DCX because the functions of the transformer are the voltage transformation and the isolation. The multicellular dc-dc converters with the regulated cell converters have been already proposed and their control stabilities have been also reported [6-10]. However, the stability issue such as the voltage imbalance among cell converters has not been discussed quantitatively in case that, the unregulated dc-dc converter is applied to the cell converter.

In Section 2, the concept of the DCX based on the multicellular converter topology is introduced. In Section 3, the behavior of the unregulated single cell converter is analyzed by using the state space averaging method, and the operating condition of the cell converter is specified to develop the multicellular

Corresponding author: Yusuke Hayashi, Ph.D., research fields: dc distribution system, dc power supply and power electronics system integration.

DCX. In Section 4, the static and the dynamic behaviors of the ISOP connected multicellular DCX are analyzed, and the voltage imbalance issue among the cell converters is discussed quantitatively. The validity of the aforementioned analyses is verified by fabricating a prototype of a 384 V-384 V 19.2 kW multicellular DCX composed of sixty-four dc-dc cell converters with the I/O (input and output) voltages of 48 V-48 V and the output power of 300 W.

2. DC-DC Transformer Based on Multicellular Converter Topology in Next Generation DC Distribution System

2.1 Configuration of Next Generation DC Distribution System for Environmentally Friendly Data Centers

The schematic illustration of the next generation dc distribution system is shown in Fig. 1. The main power distribution system consists of the following power electronics equipment:

- The front end ac-dc converter;
- The DCX;
- The POL (point of load) dc-dc converter.

The front end ac-dc converter is utilized for the interface with the ac grid and for the control of the output dc voltage. The DCX is installed for the isolation and the voltage transformation, and the function of the voltage regulation is not necessary. Equipment with various I/O voltage levels are connected via the DCX. The POL converter is installed to regulate the load voltage strictly.

In the next generation dc distribution system, the energy storages and the distributed generators based on the renewable energy sources will be installed in addition to the ICT equipment, such as the servers and the storages to realize the environmentally friendly power supply system. The input and the output voltage levels of these applications are e.g., 384 V, 192 V, 48 V and 12 V, and they have different grounding systems. The DCX for the isolation and the voltage transformation plays an important role in this system, and the high scalability of the DCX contributes to the smooth installation of a lot of renewable power sources and energy storage devices.

2.1 DC-DC Transformer Based on Multicellular Converter Topology

The multicellular converter topology is one of attractive options to discuss the feasibility of the highly efficient DCXs with various I/O voltage levels such as 384 V-12 V, 384 V-48 V and 384 V-384 V.

The concept of the multicellular DCX is shown in Fig. 2. The DCX consists of a lot of isolated dc-dc cell converters, and these cell converters are connected in types of ISOP and IPOS. The unregulated power converters are utilized as the cell converters because the DCXs are installed for the isolation and the voltage transformation. The features of the DCX are summarized as follows:

(1) The efficiency η (%) and the power density D_p (W/cm^3) of the DCX is decided by the single cell converter.

(2) The I/O voltages of the DCX are designed arbitrarily by the number of cell converters connected in series and parallel.

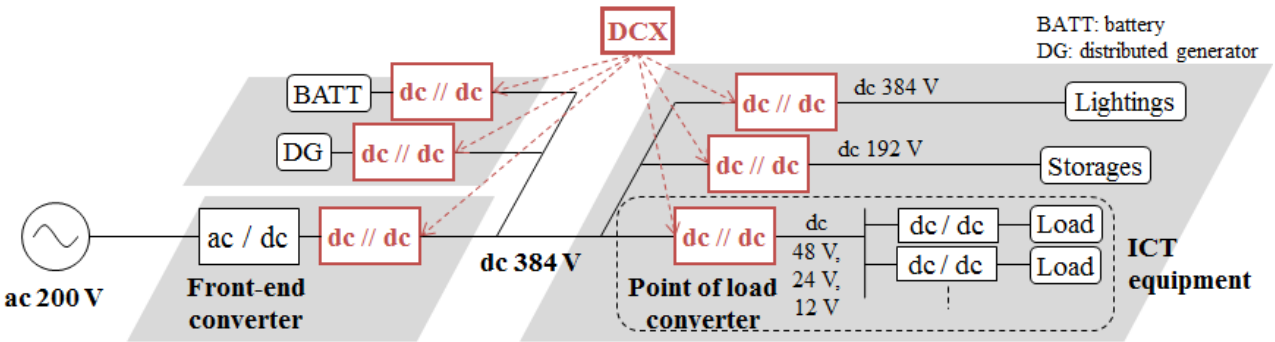

Fig. 1 Configuration of next generation dc distribution system for environmentally friendly data centers.

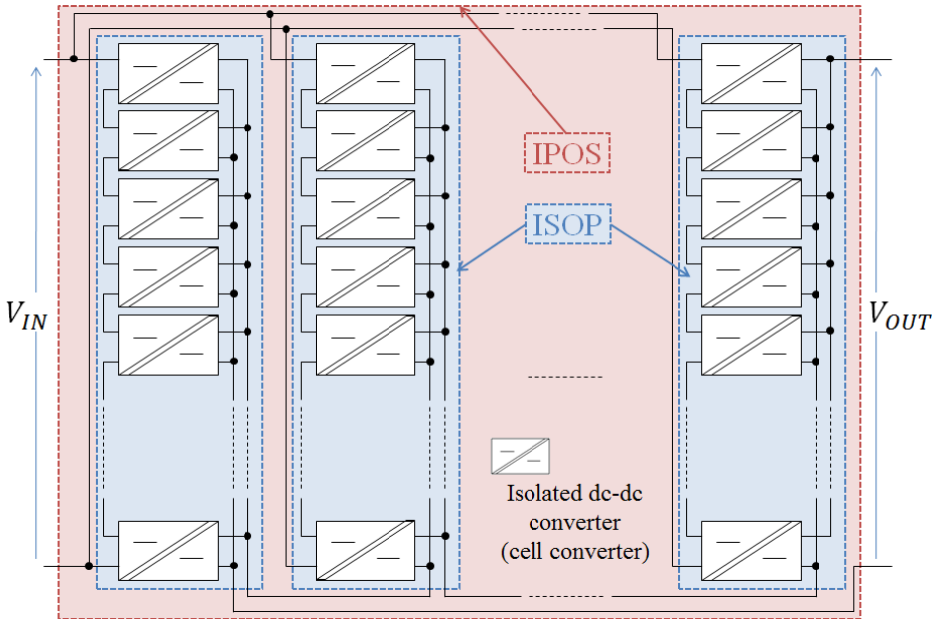

Fig. 2 Concept of multicellular DCX based on ISOP IPOS connection topology.

(3) The utilization of the unregulated dc-dc converters prevents the voltage and the current concentrations among cell converters in the steady state without any complicated control systems [11].

(4) The low voltage stress of the cell converter enables to employ the low voltage and ultralow loss semiconductor power devices [12].

The Features (1) and (2) are attractive to discuss the efficiency and the scalability of the DCX in a unified way. The Feature (4) contributes to improve the efficiency of all voltage levels of DCXs based on the multicellular converter topology.

One of key issues of the multicellular topology is the input voltage unlabance among cell converters in the ISOP connection. The Feature (3) has been already discussed qualitatively under the steady state operation condition [11]. However, the voltage imbalance in the transient state has not been described quantitatively in case that, the unregulated dc-dc converters are employed as the cell converters. In the next section, the behavior of the unregulated cell converter is analyzed by using the state space averaging method, and the operation conditions to realize the DCX is specified, taking the real circuit conditions into account.

3. Analysis of Unregulated DC-DC Cell Converter for Multicellular DC-DC Transformer

3.1 Analysis and Simplified Modeling of Single Cell Converter Based on State Space Averaging Method

The voltage imbalance among the cell converters is caused by the variation in the circuit parameters, as the choke inductor and the smoothing capacitor in each dc-dc cell converter. The dynamic response of the cell converter depends on the circuit parameters and the voltage transformation ratio varies in transient. The resonant characteristics by the circuit parameters also affect the voltage imbalance issue. In this section, the dynamic behavior of the cell converter is analyzed by using the state space averaging method [13-15] and the oeprating conditions to develop the multicellular dc-dc transformer is specified.

Fig. 3a shows the circuit configuration of an isolated buck-boost dc-dc converter. This is one of options for the single cell converter, and the instability caused by the circuit inductance and the capacitance can be discussed. Fig. 3b is the equivalent circuit of Fig. 3a in case circuit parameters are translated based on the parameters at the secondary side.

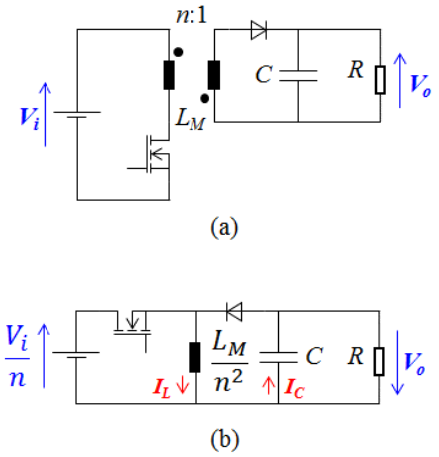

Fig. 3 Circuit configuration of (a) isolated buck-boost converter and (b) equivalent circuit.

In the case of turn ratio of the transformer $n = 1$, the behavior of the dc-dc converter is described as follows by using the state space averaging method.

$$\frac{\mathrm{d}}{\mathrm{d}t}\begin{bmatrix} i_L \\ v_o \end{bmatrix} = \begin{bmatrix} 0 & -D'/L \\ D'/C & -1/CR \end{bmatrix}\begin{bmatrix} i_L \\ v_o \end{bmatrix} + \begin{bmatrix} D/L \\ 0 \end{bmatrix} V_i \quad (1)$$

The input inductor and the output capacitor of the converter are expressed by L and C, respectively. The symbols of i_L and v_o means the input inductor current and the output capacitor voltage, respectively. The input voltage is V_i and the resistive load is R. The duty ratio of the converter is D ($D' = 1 - D$). The duty ratio D' is constant because the unregulated DCX is assumed here.

From Eq. (1), the relationship between the input and the output voltages are calculated as follows through the Laplace transformation.

$$\frac{V_o(s)}{V_i(s)} = \frac{D}{D'}\frac{1}{1 + \frac{2\delta}{\omega_0}s + \frac{1}{\omega_0^2}s^2} \quad (2)$$

$$\omega_0 = \frac{D'}{\sqrt{LC}}, \delta = \frac{1}{2D'R}\sqrt{\frac{L}{C}}$$

Eq. (2) means that, the voltage transformation ratio $V_o(s)/V_i(s)$ of the cell converter depends on the frequency of the input voltage fluctuation in the transient state. In case that, the input voltage is described as the exponential startup functions with the amplitude of unity and the time constant T_i, the output voltage can be formulated by Eq. (3).

$$V_o(s) = \frac{D}{D'} \cdot \frac{1}{1 + \frac{2\delta}{\omega_0}s + \frac{1}{\omega_0^2}s^2} \cdot \frac{1}{1 + sT_i} \cdot \frac{1}{s} \quad (3)$$

The voltage transformation ratio of the converter in the transient condition can be discussed through the inverse Laplace transformation of Eq. (3). Fig. 4 shows the calculation results of the output voltages of a 48 V-48 V 300 W buck-boost converter in case the switching frequency is varied. The detailed parameters for this calculation are summarized in Table 1. The circuit parameters L and C are designed to suppress the switching ripples of the inductor current I_L and the capacitor voltage V_o. These parameters depend on the switching frequency f_{SW} and obtained as follows.

$$L = \frac{V_L \cdot \Delta t}{\alpha \cdot I_L} = \frac{V_L \cdot D}{\alpha \cdot I_L \cdot f_{SW}} \quad (4)$$

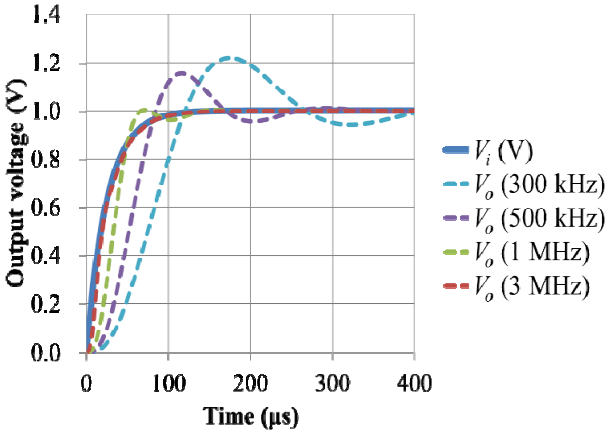

Fig. 4 Output voltages of dc-dc converters with the frequency of 300 kHz, 500 kHz, 1 MHz and 3 MHz under input voltage variation with T_i = 50 μs.

Table 1 Parameters for analysis of single cell converter.

I/O voltages V_i, V_o	48 V, 48 V			
Output power	300 W			
Inductor current i_L	6.25 A			
Duty ratio D	0.5			
Turn ratio n	1			
Time constant T_i	50 μs (correspond to 10 kHz)			
Ripple rate α, β	0.2, 0.03			
Frequency f_{SW}	300 kHz	500 kHz	1 MHz	3 MHz
Inductance L	64 μH	38.4 μH	19.2 μH	6.4 μH
Capacitance C	7.23 μF	4.84 μF	2.17 μF	0.72 μF

$$C = \frac{I_C \cdot \Delta t}{\beta \cdot V_C} = \frac{I_C \cdot D}{\beta \cdot V_C \cdot f_{SW}} \quad (5)$$

Fig. 4 means that, the high frequency converter with small L and C achieves the high responsibility. For example, the output voltage under 3 MHz switching operation precisely follows the input voltage which increases with the time constant T_i of 50 μs which corresponds to 10 kHz sinusoidal waveforms.

Fig. 5 shows the voltage transformation ratio $v_o(t)/v_i(t)$. Fig. 5 is based on Fig. 4, and the region of the constant voltage transformation ratio is extracted. In the case of 3 MHz operation, the voltage transformation ratio can be regarded as the constant value under the input voltage fluctuation with the time constant of over 50 μs. To develop the multicellular DCX, each cell converter should behave as an ideal transformer under the real circuit operation condition to avoid the complexity caused by the variation in converter parameters.

The voltage fluctuation is generally caused by the electrical system fault, the switching surge, the direct and the induced lightning surges. In the next generation dc distribution system, the lightning surges are mainly generated in the ac power feeder, and the SPDs (surge protection devices) are installed to avoid the surges. The MCCBs (molded case circuit breakers) and the SSCBs (solid state circuit breakers) are also installed to protect the power electronics devices and the ICT equipment from the electrical system faults. The DCX has to be designed taking the switching surges caused by the MCCBs and SSCBs into account.

In JEC (Japan Electrotechnical Committee)-0202-1994, the voltage waveform of the switching surge caused by the MCCB is standardized [16]. This surge is described as the impulse waveform with the time of wave front T_f is 250 μs and the time of wave tail T_t is 2,500 μs. For the SSCBs, the published datasheet gives us the transient behavior. For example, the typical turnon time of a 500 V/10 A SSCB from Crydom is 100 μs. To behave

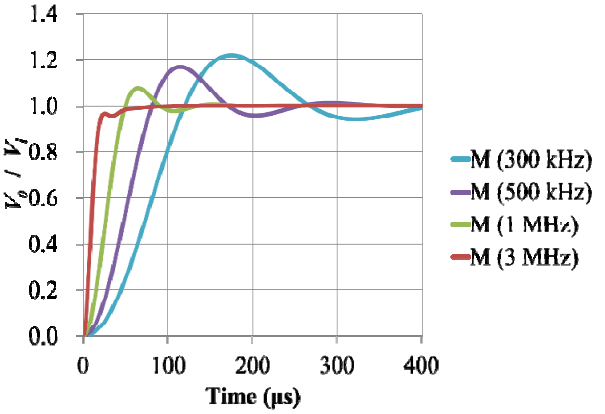

Fig. 5 Voltage transformation ratio of dc-dc converters with the frequency of 300 kHz, 500 kHz, 1 MHz and 3 MHz under input voltage variation with T_i = 50 μs.

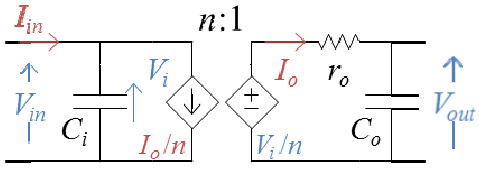

Fig. 6 Equivalent circuit of high speed single cell converter.

as the ideal transformer in the next generation dc distribution system, the operation condition with the switching frequency over MHz is required for each cell converter.

In case the cell converter operates as an ideal transformer, the equivalent circuit can be described simply as shown in Fig. 6 by using dependent voltage and current sources. This facilitates the analysis of total multicellular DCX. The validity of the equivalent circuit is confirmed in the next section.

3.2 Experimental Verification of Analysis for Single Cell DC-DC Converter

The highly efficient isolated dc-dc converters with the switching frequency of several MHz are now commercially available for the low voltage power supply. In this section, the dynamic characteristics of 3 MHz dc-dc converter (V048F480T006, VICOR) are evaluated to verify the validity of the analysis and the equivalent circuit modeling in the previous section.

Table 2 shows the parameter of the 48 V-48 V 300 W converter with the switching frequency of 3.3 MHz

Table 2 Circuit parameters for cell converter.

Rated I/O voltages (V_{in}, V_{out})	48 V, 48 V
Rated output power	300 W
Effective switching frequency	3.3 MHz
Capacitances (C_{i1}, C_{o1})	4.0 μF, 6.0 μF
Output resistance (r_{o1})	188 mΩ (max. 210 mΩ)

from VICOR. These parameters are obtained from the published datasheet. To show the dynamic response of this converter, the test circuit shown in Fig. 7 was developed. The equipment under test means the dc-dc converter, and the high speed semiconductor switch using GaN (gallium nitride) FETs (field effect transistors) with 7 mΩ from EPC (Efficient Power Conversion Corporation, Inc.) is installed to realize high speed input voltage variation.

Fig. 8a shows the experimental result of the transient response of the dc-dc converter, and Fig. 8b means the simulation result using the equivalent circuit model in Fig. 6. Figs. 8a and 8b show that, the input voltage V_{in} reaches 10 V within several μs and increases to 15 V in 15 μs with the ringing phenomenon. The output voltage V_{out} has some delay for the high speed variation before the ringing, and follows the input voltage V_{in} after 5 μs. The simulation result based on Fig. 6 has

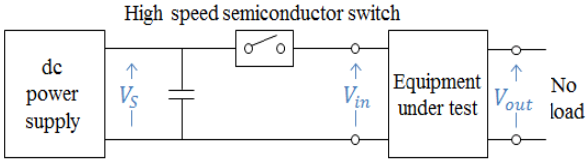

Fig. 7 Test circuit for transient response measurement.

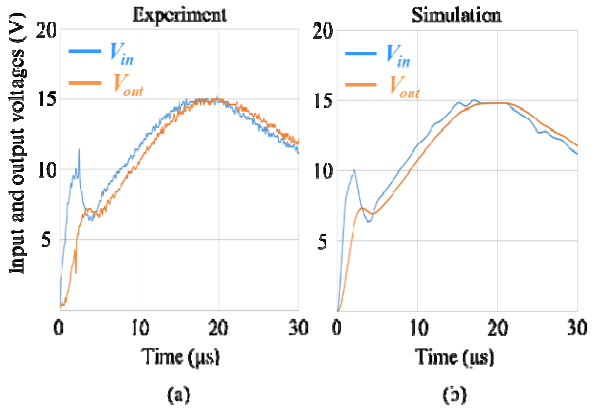

Fig. 8 Transient response of high speed unregulated dc-dc converter: (a) experiment (b) circuit simulation PSIM.

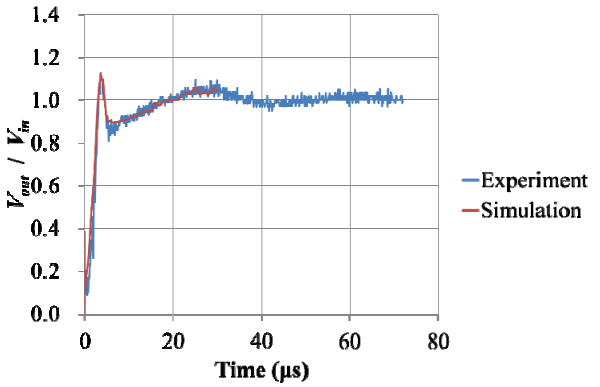

Fig. 9 Voltage transformation ratio V_{out}/V_{in} of dc-dc converter: (a) experiment (b) circuit simulation by PSIM.

good agreement with the experiment and this model can be utilized for the multicellular DCX analysis.

Fig. 9 shows the voltage transformation ratio V_{out}/V_{in} of the dc-dc converter. After 50 μs, the transformation ratio converges to the constant value 1 and this result also corresponds to the calculation result shown in Fig. 5.

4. Analysis and Prototyping of Multicellular DC-DC Transformer

4.1 Transient Analysis of Multicellular DC-DC Transformer

From the aforementioned analysis, the voltage transformation ratio can be regarded as a constant value for the unregulated dc-dc converters, whose switching frequency is over MHz in case the input voltage varies with the time constant over 50 μs. Although the switching surge of 100 μs caused by the solid state circuit breaker is the critical issue in the next generation dc distribution system, the MHz operated unregulated dc-dc converter behaves as an ideal transformer for the surge.

Generally, the transient analysis of the multicellular DCX is complicated in case the cell converters with the variable transformation ratios are employed. The aforementioned high speed cell converter facilitates this analysis and the voltage imbalance among cell converters can be discussed quantitatively.

Fig. 10 shows the circuit configuration of the multicellular DCX which consists of two cell

converters connected in ISOP. Each cell converter is described by using the dependent voltage and the current sources with the voltage transformation ratio 1. The input and the output voltages of the multicellular transformer are V_{in} and V_{out}, respectively. The input voltages of cell converters are V_{i1} and V_{i2}. Input capacitors of cell converters are C_{i1} and C_{i2}. The symbols of C_{o1} and C_{o2} are the output capacitances of cell converters, and these capacitors are bundled with C_o. The total load resistance is $R_o/2$ (R_o corresponds to the rated output power of each cell converter) and the output resistances of cell converters are r_{o1} and r_{o2}. The circuit parasitic inductances are not considered here because the parasitic inductances are negligible in the highly integrated low voltage converters.

The relationships between the voltages and the currents in Fig. 10 are formulated as Eqs. (6)-(12).

$$V_{in} = V_{i1} + V_{i2} \tag{6}$$
$$V_{i1} = V_{out} + r_{o1} \cdot I_{o1} \tag{7}$$
$$V_{i2} = V_{out} + r_{o2} \cdot I_{o2} \tag{8}$$
$$V_{out} = R_o/2 \cdot I_{out} \tag{9}$$
$$I_{in} = I_{o1} + sC_{i1} \cdot V_{i1} \tag{10}$$
$$I_{in} = I_{o2} + sC_{i2} \cdot V_{i2} \tag{11}$$
$$I_{out} = I_{o1} + I_{o2} - sC_o \cdot V_{out} \tag{12}$$

From Eqs. (6)-(12), the relationship between the input voltage of the multicellular converter V_{in} and the input voltage of the single cell converter V_{i1} is formulated as follows:

$$\frac{V_{i1}}{V_{in}} = \frac{s^2 r_{o1} r_{o2} C_{i2} C_o + sK_2 + 2\left(1 + \frac{r_{o1}}{R_o}\right)}{s^2 r_{o1} r_{o2} (C_{i1} + C_{i2}) C_o + sK_1 + 2^2 \left(1 + \frac{r_{o1} + r_{o2}}{2R_o}\right)} \tag{13}$$

where,

$$K_1 = \left\{(r_{o1} + r_{o2})(C_{i1} + C_{i2}) + C_o(r_{o1} + r_{o2}) + \frac{2r_{o1}r_{o2}}{R_o}(C_{i1} + C_{i2})\right\}$$

$$K_2 = \left\{(r_{o1} + r_{o2})C_{i2} + r_{o1}C_o + \frac{2r_{o1}r_{o2}C_{i2}}{R_o}\right\}$$

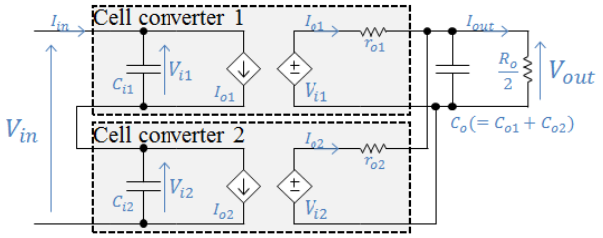

Fig. 10 Configuration of multicellular dc-dc transformer connected in ISOP.

From Eq. (13), the input cell voltage V_{i1} in the steady state can be calculated by using the final value theorem. Here, V_{in} is expressed by the exponential startup function with the time lag τ.

$$\lim_{S\to 0} s\,V_{i1} = \frac{1}{2} \cdot \frac{1 + \frac{r_{o1}}{R_o}}{1 + \frac{r_{o1} + r_{o2}}{2R_o}} \cdot \frac{1}{1 + s\tau} \cdot \frac{1}{s} \cdot \mathrm{s} = \frac{1}{2} \cdot \frac{1 + \frac{r_{o1}}{R_o}}{1 + \frac{r_{o1} + r_{o2}}{2R_o}} \tag{14}$$

The input cell voltages have the imbalance caused by the output resistances r_{o1}, r_{o2} and the load resistance R_o. However, the output resistances r_{o1}, r_{o2} are significantly smaller than the load resistance R_o and the input cell voltages V_{i1}, V_{i2} are approximately divided equally. This equation means that, the utilization of the unregulated dc-dc converters contribute to preventing the voltage concentrations among cell converters without any complex controls.

Fig. 11 shows the calculation result of the input cell voltages in case that, the input voltage of the multicellular transformer increased with the time lag τ. Parameters for this calculation is shown in Table 3. The utilization of the commercially available high speed dc-dc converters (V048F480T006, VICOR) was assumed. The circuit parameters in Table 3 are based on the parameters in Table 2 and the additional input capacitors are installed for each cell converter.

In case that, the input voltage of the multicellular DCX V_{in} is varied as the ideal step function, the imbalance between the input cell voltages V_{i1} and V_{i2} occurs because of the mismatch of the cell converter input capacitances C_{i1} and C_{i2}. In case that, the voltage V_{in} varies with the time constant τ more than 5 μs, the

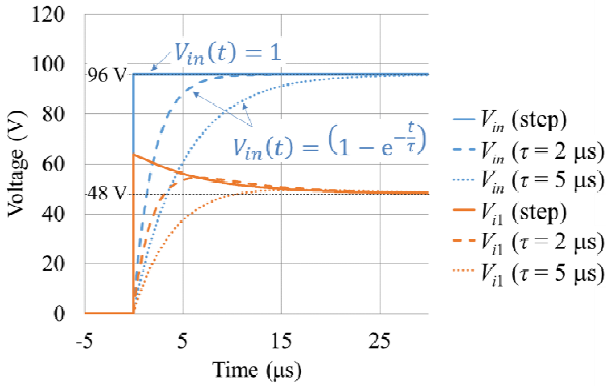

Fig. 11 Calculated input voltages of cell converter in case input voltage of multicellular dc-dc transformer varied with time constant τ.

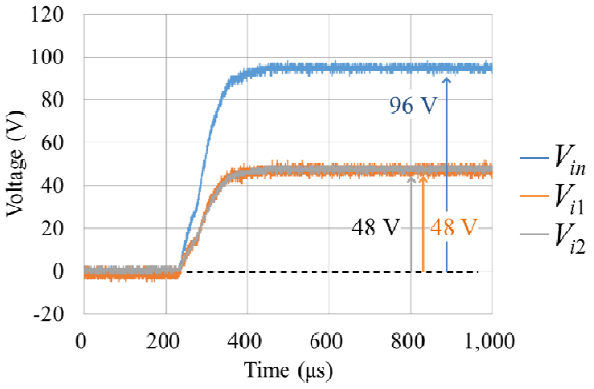

Fig. 12 Input voltage sharing between two cell converters in case input voltage increased with time constant of 100 μs.

Table 3 Parameters for voltage imbalance calculation for two cell converters connected in ISOP.

Input voltage V_{in}	DC 96 V for 2 cells
Output voltage V_{out}	DC 48 V
Output resistance r_{o1}, r_{o2}	188 mΩ
Input capacitance C_{i1}, C_{i2}	26 (= 22 + 4) μF, 48 (= 44 + 4) μF
Output capacitance C_o	12 μF (= 6 μF + 6 μF)

voltage V_{i1} follows half of V_{in} without any overshoot. Under the real operation condition with the time constant τ over 50 μs shown in the previous section, the input voltage of each cell converter balances in the transient state.

The experimental result of the input voltage sharing is shown in Fig. 12. Parameters for this experiment are based on Table 3. Two dc-dc converters of V048F480T006 were connected in ISOP as shown in Fig. 10. The input voltage V_{in} reached 96 V in 100 μs and the rise time of 100 μs depended on the commercially available 500 V/10 A solid state circuit breaker (D5D10, Crydom). In Fig. 12, the input voltages of two cell converters V_{i1} and V_{i2} varied from 0 V to half of 96 V without any imbalances. This result corresponded to the aforementioned estimation and the validity of the analysis for the multicellular DCX was verified.

4.2 Prototype of 384 V-384 V 19.2 kW Multicellular DC-DC Transformer

The dc-dc cell converters with the switching frequency over MHz solve the voltage imbalance problem in the multicellular converter topology under the real circuit operation condition in the next generation dc distribution system. In this section, the prototype of a 384 V-384 V 19.2 kW DCX using V048F480T006s from VICOR is introduced.

The 384 V-384 V DCX consists of sixty-four unregulated cell converters. Eight cell converters develop a 384 V-48 V ISOP connected DCX unit and eight units makes a 384 V-384 V IPOS connected DCX. The image of the transformer is illustrated in Fig. 2. The total output power of the 384 V-384 V DCX is 19.2 kW because the output power of single cell converter is 300 W.

The fabricated DCX unit with the voltage levels of 384 V-48 V is shown in Fig. 13. Eight cell converters of V048F480T006 are embedded with the external input capacitors and the gate power supplies. The developed 384 V-384 V DCX using the eight units is shown in Fig. 14. The total volume of the transformer is about 2,000 cm^3 for 19.2 kW output power. Parameters for the DCX are summarized in Table 4.

Fig. 15 shows the startup operation of the DCX under the no load condition. The input and the output voltages for one of 384 V-48 V DCX units are shown. The rise time of the 384 V input is about 100 ms because of the soft starting function of the dc voltage source. The rise time is significantly slow for the cell converters, the output voltage of the DCX unit is in proportion to the input voltage. The input voltages of

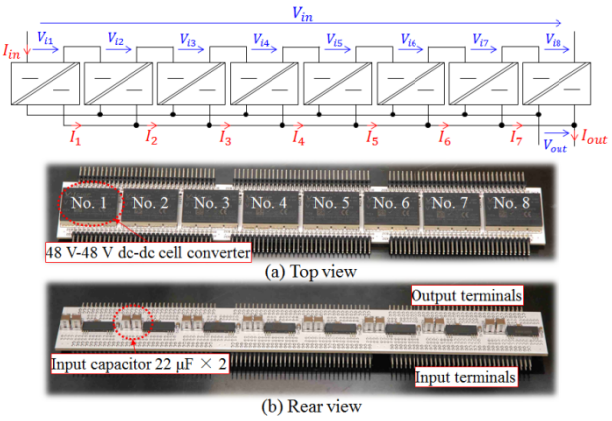

Fig. 13 ISOP connected 384 V-48 V dc-dc transformer unit using eight cell converters.

Table 4 Parameters for multicellular dc-dc transformer.

384 V-384 V dc-dc transformer	
Input voltage	dc 384 V
Output voltage	dc 384 V
Output power	19,200 W
Number of ISOP units	8
384 V-48 V ISOP connected dc-dc transformer unit	
Input voltage	dc 384 V
Output voltage	dc 48 V
Output power	2,400 W
Number of cell converters	8
48 V-48 V dc-dc cell converter	
Model number	V048F480T006 (VICOR)
Input voltage	dc 48 V
Output voltage	dc 48 V
Output power	300 W (rated)
Output resistance	188 mΩ (max. 210 mΩ)
External input capacitance	44 μF ± 20% MLCC (multilayer ceramic capacitor)

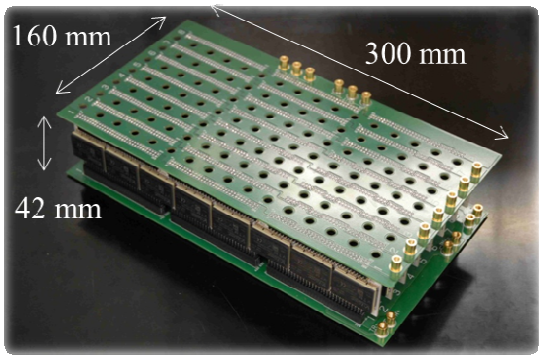

Fig. 14 ISOP IPOS connected 384 V-384 V 19.2 kW dc-dc transformer using sixty-four cell converters.

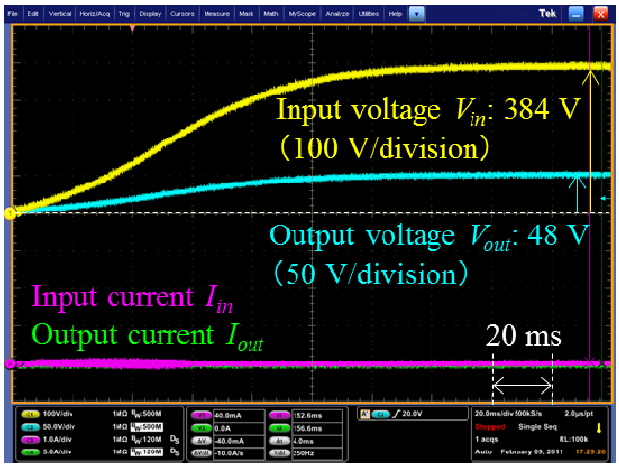

Fig. 15 Startup operation of multicellular dc-dc transformer.

cell converters approximately correspond to the output voltage, because cell converters are connected in ISOP and their voltage transformation ratio are 1.

Fig. 16 shows the voltage and the current waveforms for two cell converters under the rapid load variation. The load current increases from 0% to 100% in 1 ms and also decreases from 100% to 0% in the same speed. Fig. 16 shows that, the input voltages of cell converters balanced and these voltages converge 48 V (= 384 V/8) in the rapid load variation. Fig. 16 also shows that, the output current of each cell converter balances. The output current of 38.8 A means the total current of six cell converters from No. 1 to No. 6 in Fig. 13. The output current of 32.4 A means the total current of five cell converters. The output current of single cell converter is estimated as 6.3 A by subtracting them, and the current of 6.3 A is approximately equal to the rated current of 6.25 A for the single cell converter (6.25 A = 300 W/48 V).

Finally, the conversion efficiency of the multicellular DCX and the single cell converter are shown in Fig. 17. The horizontal axis is the output power ratio for the rated power. Here, the rated power of 100% means 19.2 kW for the multicellular transformer and the power of 100% means 300 W for the single cell converter. The efficiency of the DCX has good

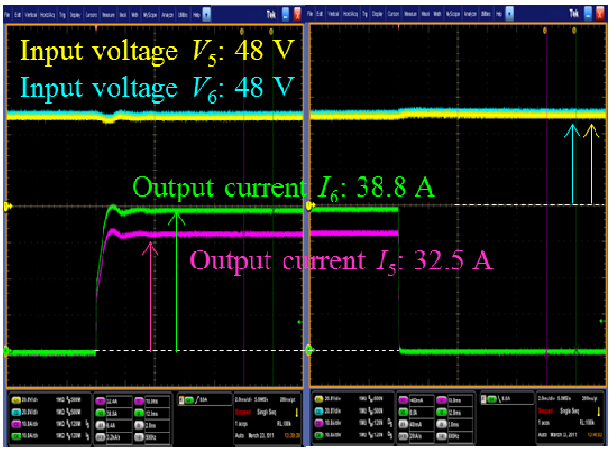

Fig. 16 Rapid load variation for multicellular dc-dc transformer.

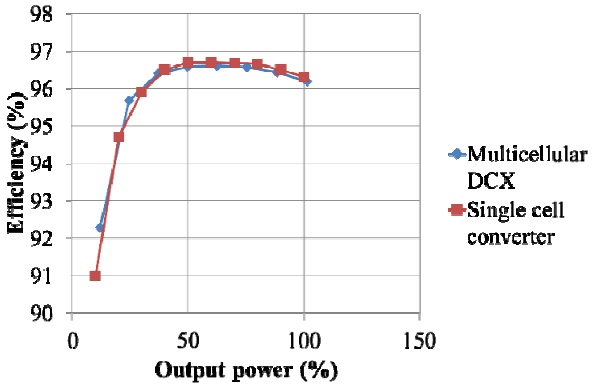

Fig. 17 Efficiencies of multicellular dc-dc transformer and single cell converter.

agreement with the efficiency of the single cell converter, and the scalability of the multicellular converter topology is demonstrated.

5. Conclusions

A multicellular DCX using unregulated cell converters was proposed for the environmentally friendly data centers. The analysis of the single cell converter based on the state space averaging method showed that, high speed cell converter with the switching frequency over MHz behaves as an ideal transformer, and this behavior solves the voltage imbalance issue in the multicellular converter topology. The behavior of the multicellular DCX using the high speed cell converters was also analyzed, and the voltage imbalance issue among cell converters was discussed quantitatively. The validity of the analyses was verified by fabricating a prototype of a 19.2 kW 384 V-384V multicellular DCX using sixty-four unregulated cell converters.

References

[1] Schmidt, R. R., Belady, C., Classen, A., Davidson, T., Herrlin, M. K., Novotny, S., and Perry, R. 2004. "Evolution of Data Center Environmental Guidelines." *ASHRAE Transactions* 110 (1): 559-66.

[2] Ministry of Internal Affairs and Communications. 2014. "2014 White Paper Information and Communications in Japan." Ministry of Internal Affairs and Communications.

[3] Sugiyama, Y. 2011. "Green ICT toward Low Carbon Society-Green R & D Activities in NTT." Presented at the 4th International Workshop on Green Communications, Kyoto, Japan.

[4] Yamasaki, M., Kanai, T., Mino, M., and Ohashi, H. 2011. "Potentialities and Problems of the SiC Devices to Apply Practical Use." Presented at the Japan Industry Applications Society Conference, Okinawa, Japan.

[5] Ninomiya, T., Ishizuka, Y., Shibahara, R., and Abe, S. 2012. "Energy-Saving Technology Using Next-Generation Power Electronics." In *Proceedings of the IEE (Institution of Electrical Engineers)-Japan Industry Applications Society Conference,* I15- I20.

[6] Ayyanar, R., Giri, R. and Mohan, N. 2004. "Active Input-Voltage and Load-Current Sharing in Input-Series and Output-Parallel Connected Modular DC-DC Converters Using Dynamic Input-Voltage Reference Scheme." *IEEE Trans. on Power Electronics* 19 (6): 1462-73.

[7] Wang, L., and He, X. 2007. "Input-Series and Output-Parallel Connection Modular DC-DC Converters with Interleaved Constant Duty Cycle Control Strategy." In *Proceedings of the 33rd Annual Conference of the IEEE Industrial Electronics Society (IECON),* 1901-6.

[8] Kimball, J., Mossoba, J., and Krein, P. 2008. "A Stabilizing, High-Performance Controller for Input Series-Output Parallel Converters." *IEEE Trans. on Power Electronics* 23 (3): 1416-27.

[9] Kim, J., You, J., and Cho, B. 2001. "Modeling, Control, and Design of Input-Series-Output-Parallel-Connected Converter for High-Speed-Train Power System." *IEEE Trans. on Industrial Electronics* 48 (3): 536-44.

[10] Kasper, M., Chen, C., Boris, D., Kolar, J., and Deboy, G. 2015. "Hardware Verification of a Hyper-Efficient (98%) and Super-Compact (2.2 kW/dm^3) Isolated AC/DC Telecom Power Supply Module Based on Multi-cell Converter Approach." In *Proceedings of the IEEE Applied Power Electronics Conference and Exposition (APEC),* 65-71.

[11] Hayashi, Y., and Masato, M. 2014. "An Approach to a Higher-Power-Density Power Supply for 380-V DC

Distribution System." *Electrical Engineering in Japan* 186 (3): 51-62.

[12] Tolbert, L. M., Ozpineci, B., Islam, S. K., and Chinthavali, M. S. 2003. "Wide Bandgap Semiconductors for Utility Applications." In *Proceedings of the IASTED (International Association of Science and Technology for Development) International Conference on PES (Power and Energy Systems) 2003,* 317-21.

[13] Erickson, W., and Maksimovic, W. 2001. *Fundamentals of Power Electronics.* New York: Springer US.

[14] Middlebrook, R., and Cuk, S. 1976. "General Unified Approach to Modeling Switching-Converter Power Stages." In *Proceedings of the IEEE Power Electronics Specialist Conference (PESC),* 18-34.

[15] Ninomiya, T., Nakahara, M., Higashi, T., and Harada, K. 1991. "Unified Analysis of Resonant Converters." *IEEE Trans. on Power Electronics* 6 (2): 260-70.

[16] Japanese Electro-technical Committee. 1995. "Impulse Voltage and Current Tests in General." Japanese Electro-technical Committee.